Reversible Underwater Lossless Oil Droplet Transportation

Jiale Yong, Qing Yang, Feng Chen,* Hao Bian, Guangqing Du, Umar Farooq, and Xun Hou*

The controllable transportation of microdroplets has attracted considerable interest because of its wide range of promising applications in biochemical separation, bioadhesion, in situ analysis, in situ detection, and lab-on-chip devices.[1–6] Most previous efforts to control liquids have been focused on the design of complicated micromechanical components, such as micropumps, microchannels, microvalves, and microsensors.[7–10] However, the use of common solid materials in these applications results in surface contamination and droplet losses that are unavoidable because of droplet wetting, pinning, and contact angle hysteresis.[7] Therefore, the generation of a functional surface for controlling microdroplet transportation by a simple and practical approach is greatly needed. Specifically, with the fast development of superhydrophobic materials as well as skillful wettability control techniques, it is possible to realize two extremely superhydrophobic states: ultralow water adhesion and ultrahigh water adhesion, which are inspired by the lotus leaf and the rose petal, respectively.[11–13] As a result, water droplets can roll down freely from the substrate without any liquid residues or be pinned to the surface in a controlled fashion. From this basis, superhydrophobic surfaces are considered to be potential candidates for no-loss transportation of water droplets.[14,15] For example, Jiang and co-workers[16,17] fabricated a superhydrophobic aligned polystyrene nanotube layer via a porous alumina membrane covering method. The fabricated surface exhibited a strong adhesive force to water and could be easily used to transfer a water droplet from a superhydrophobic surface to a superhydrophilic one with no volume loss. Later, they presented an in situ control of superparamagnetic microdroplets by manipulating the external magnetic field, thereby achieving transportation of superparamagnetic microdroplets.[18,19] Sun and co-workers[20] reported a novel curvature-driven in situ switching between pinned and roll-down superhydrophobic states on polydimethylsiloxane micropillar arrays, that is, the water adhesion of the surface was reversibly switched from ultralow to ultrahigh by tuning the surface curvature. In this way, the surface could function as a mechanical hand for water microdroplet "pickup" when flat and "release" when at a certain curvature.

Dr. J. Yong, Prof. Q. Yang, Prof. F. Chen, Dr. H. Bian, Dr. G. Du, U. Farooq, Prof. X. Hou
State Key Laboratory for Manufacturing System Engineering and Key Laboratory of Photonics Technology for Information of Shaanxi Province
Xi'an Jiaotong University
Xi'an 710049, P.R. China
E-mail: yangqing@mail.xjtu.edu.cn; chenfeng@mail.xjtu.edu.cn

DOI: 10.1002/admi.201400388

In addition to the water–air–solid system that analyzes water droplets and superhydrophobic surfaces, there has been much recent interest in the interface of liquid oil, another important liquid in our daily life, and solids.[21–24] Jiang and co-workers[25] found that fish can swim freely and keep their skin clean even in the oil-polluted water. They revealed that this special ability is caused by the underwater superoleophobicity of fish scales, which is a result of the hydrophilic chemistry of fish scales and their hierarchical rough structures. According to the modified Cassie's theory, water can be trapped in the hierarchical rough structure to form a repulsive oil layer, resulting in an oil–water–solid interface.[25–28] The trapped water layer endows the surface with superoleophobicity and ultralow oil-adhesion in water. The underwater superoleophobic surfaces have some fascinating practical applications in marine antifouling, bioadhesion, water/oil separation, and microfluidic technologies.[28–37] Although some strategies have been developed to manipulate water droplets in air with superhydrophobic surface, finding a simple route for the controllable transportation of oil microdroplets without mass loss in water has remained challenging.

Here, we report for the first time a simple and novel method to in situ transfer oil droplets in water based on superoleophobic surfaces and switching the density of the water solution. Femtosecond laser-irradiated silicon surfaces show a micro/nanoscale hierarchical structure and underwater superoleophobicity with ultralow oil-adhesion. An oil droplet can be picked up when the density of the water solution surrounding the oil droplet is larger than that of the oil by adding sugar to water, which causes the buoyancy acting on the oil droplet to be larger than the gravity. The oil droplet can also be put down when the density of water solution is lower than that of the oil droplet; this is accomplished through dilution. Based on this unique switching, an in situ "mechanical hand" for no-loss oil droplet transportation was realized in a water environment.

The rough micro/nanoscale structure was formed by femtosecond laser irradiation using a line-by-line and serial scanning process. The details of the experimental setup and the scanning method are described in our previous work.[38–40] A p-type silicon wafer was irradiated by a regenerative amplified Ti:sapphire laser system (pulse duration: 50 fs; center wavelength: 800 nm; repetition: 1 kHz). The laser beam (constant average power of 20 mW) was focused on the sample by a microscope objective lens (NA = 0.45). The sample was irradiated at scanning speed of 2 mm s^{-1} and interval of adjacent laser scanning lines of 2 μm.

Figure 1 shows scanning electron microscopy (SEM) images of the femtosecond laser-scanned silicon surface. The as-prepared surface was constructed by periodic rough micromountain array with the period of about 10 μm. Each micromountain has a diameter of about 6 μm and a height of about 2.9 μm. In general, there are four holes around a single micromountain.

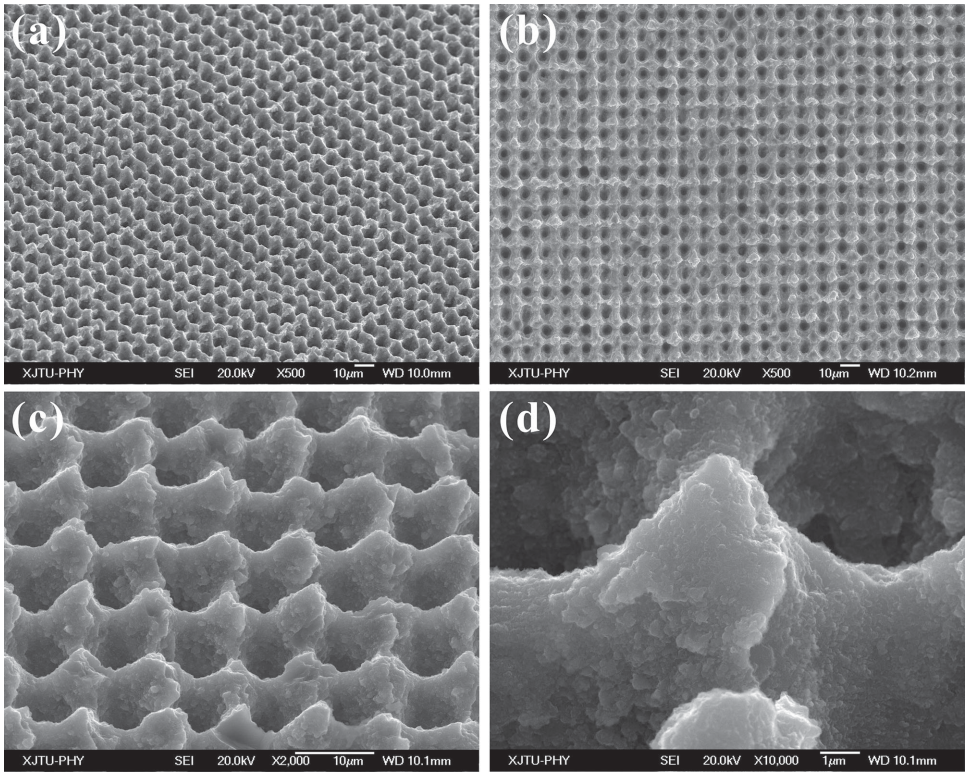

Figure 1. SEM images of the femtosecond laser-irradiated silicon surface. a) 45° tilted view, b) top view, c) higher resolution 45° tilted view, and d) large-magnification SEM image of a single micromountain decorating with nanoscale protrusions.

High-magnification SEM imaging reveals that the micromountains are randomly decorated with many irregular nanoscale protrusions (Figure 1d). The micro/nanoscale hierarchical rough structures are believed to develop from ablation under laser pulses and the recrystallization of ejected particles. The roughness (*Ra*) of the as-prepared surface is about 2.2 μm. This rough micro/nanoscale binary structure is helpful to realize superhydrophilicity in air and underwater superoleophobicity.

Previous research has demonstrated that superhydrophilicity of a solid surface in air is important for achieving underwater superoleophobicity.[28,29] For a flat silicon surface, hydrophilicity is exhibited with a water contact angle (WCA) of about 60° in air and ordinary oleophobicity with an intrinsic oil contact angle (OCA) of 125.5° ± 2° in water (**Figure 2**a). After introducing a rough structure by femtosecond laser irradiation, the samples change from exhibiting hydrophilicity to superhydrophilicity in air. A water droplet will spread out quickly on the laser-induced surface once it is placed on the surface, leading to a small WCA of about 2.5°, as shown in Figure 2b. Figure 2c describes the shape of an 8-μL oil droplet deposited on the laser-irradiated surface in water. At this time, the oil droplet shows an approximately spherical shape. The OCA is measured to be 160.2° ± 1°, indicating an underwater superoleophobic character. Figure 2d presents the process of an underwater oil droplet rolling off on a 0.5°-tilted as-prepared surface under the gravitation effect (Movie S1, Supporting Information). This result shows that there is ultralow oil-adhesion between the oil droplet and the laser-irradiated surface in water. The adhesive force measured was only about 1.3 μN. Based on the high OCA value and the ultralow oil-adhesion, the underwater oil droplet on the laser-irradiated surfaces can be considered to be in the Cassie state.[25,26]

It is generally known that a hydrophilic surface in air becomes oleophobic in water, whereas the hierarchical rough structure can significantly amplify the superoleophobicity.[28,29] Silicon is an intrinsically hydrophilic material in air. After femtosecond laser irradiation, the surface becomes superhydrophilic in air because of the generated micro/nanoscale binary rough structure. Once such a surface is immersed in water, the water will immediately enter into and occupy all of the interspaces between the microstructures. A water cushion is thus formed below the oil, causing the oil droplet to sit on the top of the rough microstructure. According to a generalized version of Cassie's model, the oil droplet resides on a composite solid–water interface, forming an oil–water–solid three-phase system.[25,26] The trapped water layer offers a strong repulsive force to the oil droplet due to repulsive interaction between polar (water) and nonpolar (oil) molecules, endowing the as-prepared surfaces with underwater superoleophobicity.[41] In addition, the hierarchical microstructure can effectively reduce the contact area between the oil droplet and the silicon surface. As a result, the as-prepared surface exhibits small adhesive force and ultralow oil-adhesion.

To take advantage of the ultralow oil-adhesion of underwater superoleophobic surfaces, we propose an in situ "mechanical hand" for no-loss oil droplet transportation in water by switching the density of water solution surrounding the oil

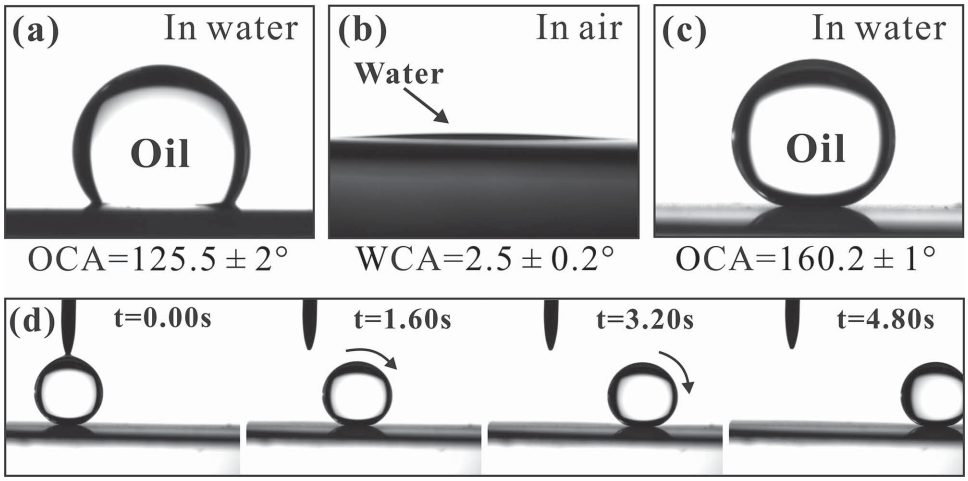

Figure 2. Wettable properties of the surface before and after femtosecond laser irradiation. a) The shape of an oil droplet on the untreated silicon surface in water. b,c) The shapes of a water droplet and an oil droplet on the femtosecond laser-irradiated surface in air and in water, respectively. The underwater oil droplet on the as-prepared surface shows superoleophobicity with OCA of 160.2° ± 1°. d) Time sequence of an oil droplet rolling on the 0.5° tilted as-prepared surface, showing an ultralow oil-adhesion.

droplet. The setup is schematically shown in **Figure 3**a. As seen in Figure 3b and Movie S2 (Supporting Information), an as-prepared sample was lowered down until it made contact with the oil droplet on another as-prepared sample (Steps 1–3). When the above-sample was lifted up, the oil droplet continued to sit on the below-sample due to gravity (Steps 3–5) and the untreated water. On the contrary, by changing the liquid surrounding the oil droplet from water-to-water solution by adding sugar, the density of water solution becomes greater than that of oil, and the buoyancy would be able to combat the gravity. This switching of the density of water solution may provide the possibility for in situ transportation of oil droplet in water. Sugar was selected to increase the density of water solution because it has many advantages, such as nontoxicity, environment friendly, large solubility in water, and insolubility with oil. In order to speed up the transportation process, sugar water with a density of about 1.52 g cm^{-3} was prepared in advance by dissolving sugar into deionized water.

Figure 3c shows the detailed process of underwater oil droplet transportation (Movie S3, Supporting Information). A 15-μL oil droplet with a density of 1.26 g cm^{-3} was initially placed on an as-prepared superoleophobic sample (below-sample) in water (Step 1). Then, another as-prepared sample (above-sample) was lowered down until it made contact with the oil droplet (Step 2). At this point, the sugar water with a density of 1.52 g cm^{-3} was poured into the glass container slowly until the color of the water solution was at or near the color of the sugar water, a pale green-yellow (Step 3). This process switched the density of water solution from lower than that of the oil to larger than that of the oil. Simultaneously, the image of the underwater oil droplet became brighter because the refractive index of sugar water is closer to that of oil droplet than that of deionized water. By lifting the above-sample up, the oil droplet was elevated with the above-sample and shifted from the below-sample to the above-sample because the buoyancy was larger than the gravity (Step 4). Surprisingly, the oil droplet could be put back on the below-sample. The above-sample was lowered down again until the hanging oil droplet made contact with the below-sample (Step 5). Next, deionized water with density of 1 g cm^{-3} was added into the glass container. The water solution in the container was diluted until its color changed to very clear and transparent, indicating that the density of water solution was close to that of deionized water (Step 6). The image of oil droplet returned to its original brightness. At this point, the density of water solution was much less than that of the oil droplet. Finally, when lifting the above-sample up, the oil droplet was detached from above-sample and stayed on the below-sample (Step 7). In this way, the oil droplet can be in situ transferred between the below-sample and the above-sample, as shown in Figure 3d. Furthermore, this reversible transportation could cycle a large number of times by switching the density of water solution, demonstrating excellent reproducibility and stability (Figure 3e). In general, an oil droplet usually presents a quasi-spherical shape on superoleophobic surface, and the contact area between the oil droplet and the sample is significantly reduced. Therefore, the transportation process causes almost no loss of microdroplet for a small contact area and ultralow oil-adhesion. We believe that our in situ oil transportation exhibits great potential for biomedical and microfluidic devices.

An oil droplet also can be transferred to a higher place using the above-mentioned method, as shown in **Figure 4** and Movie S4 (Supporting Information). An oil droplet was first put on an as-prepared superoleophobic surface (A-surface) in water (Figure 4a). Then, another as-prepared surface (B-surface) was lowered down until it made contact with the oil droplet (Figure 4b). The sugar water was subsequently poured into the glass container until the image of the underwater oil droplet became brighter (Figure 4c). As seen in Figure 4d, the oil droplet was detached from A-surface and rose with the B-surface as it lifted up because the buoyancy acting on the oil droplet was larger than the gravity. Next, the A-surface was removed and another superoleophobic surface (C-surface) was moved to a location below the B-surface by at a higher altitude than the original A-surface (Figure 4e). The B-surface was lowered

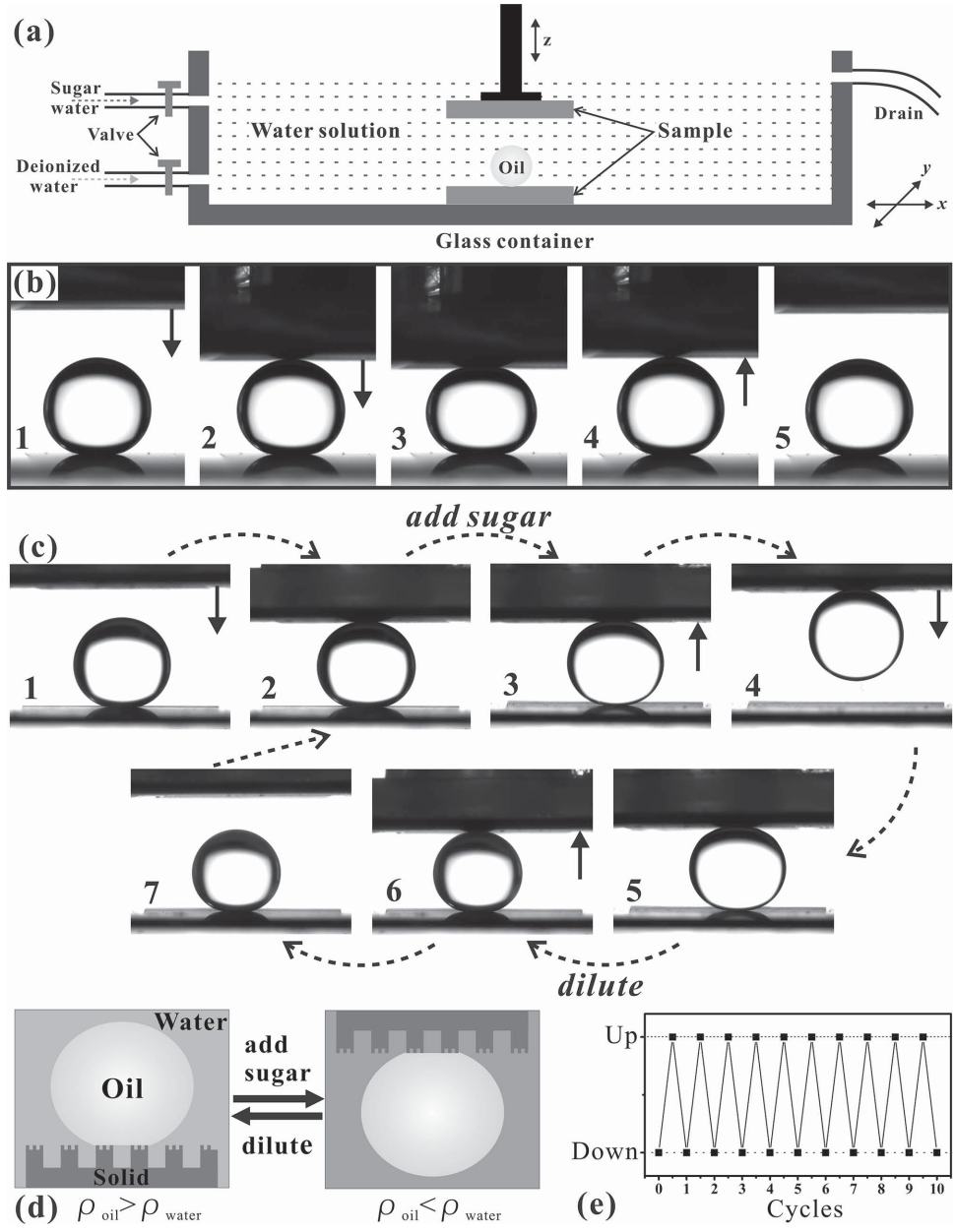

Figure 3. In situ transportation of an oil droplet in water based on superoleophobic surfaces with ultralow oil-adhesion and the switching of the density of the water solution. a) Schematic illustration of the setup. b) An as-prepared sample making contact with and leaving the oil droplet on another as-prepared sample when the water in the glass container was untreated. c) Detailed working process of no-loss oil droplet transportation in water (see text for detailed explanation). d) Schematic illustration and e) reversibility test of the oil droplet being switched between "put down" and "pick up" states.

down again until the hanging oil droplet made contact with the C-surface (Figure 4f). Then, the water solution was diluted by adding deionized water into the glass container until the density of the water solution was close to that of deionized water (Figure 4g). Finally, the oil droplet was detached from B-surface and shifted to the C-surface by lifting the B-surface up as seen in Figure 4h. In this way, the water droplet was moved from A-surface to a higher C-surface simply by switching the density of water solution.

In conclusion, simple in situ transportation of oil droplets in water based on superoleophobic surfaces with ultralow oil-adhesion and the switching of the density of the water solution has been demonstrated for the first time. Silicon surfaces with micro/nanoscale hierarchical structures were fabricated by femtosecond laser irradiation. The as-prepared surfaces show underwater superoleophobicity with ultralow oil-adhesion. The density of water solution surrounding the oil droplet can be made larger than or lower than the oil by adding sugar to water or diluting the solution with pure deionized water, respectively. At the same time, the buoyancy acting on the oil droplet will be larger than or smaller than the gravity of oil droplet. This reversible switching endows the superoleophobic surface with

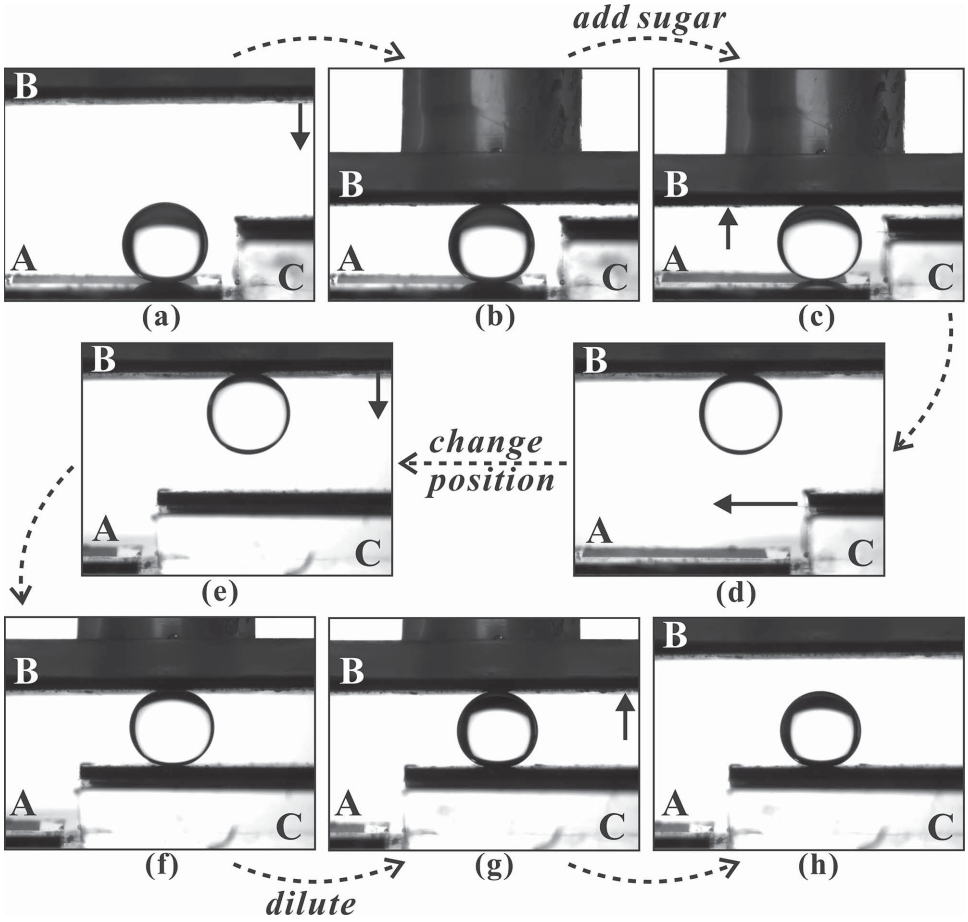

Figure 4. Transportation process of an oil droplet from the A-surface to the higher C-surface via the B-surface.

the ability of "pick up" and "put down" the oil droplet in water. As a result, an in situ mechanical hand for no-loss oil droplet transportation was realized. This subtle control of underwater oil droplet mobility provides a new insight into smart superoleophobic surfaces, and we believe that potential applications will emerge in the biological and microfluidic fields.

Experimental Section

Materials: Single crystal p-type Si (100) wafer was mounted on a motorized stage controlled by computer. A regenerative-amplified Ti:sapphire laser system (CoHerent, Libra-usp-1K-he-200) with pulse duration of 50 fs, center wavelength of 800 nm, and repetition of 1 kHz was utilized. The laser beam (constant average power of 20 mW) was focused on the sample using a microscope objective lens (20×, NA = 0.45, Nikon). A line-by-line and serial scanning process was adopted. The sample was irradiated at the scanning speed of 2 mm s^{-1} and the interval of adjacent laser scanning lines of 2 μm. After laser irradiation, the samples were successively cleaned by acetone, alcohol, and deionized water in ultrasonic bath for 10 min, respectively.

Characterization: The surface morphology of the samples was analyzed by a JSM-7000F scanning electron microscope (JEOL, Japan). The static contact angles of an 8-μL water or oil droplet were carried out using a JC2000D4 contact-angle system (POWEREACH, China), and average values were measured five different points on the same surface. 1,2-dichloroethane ($C_2H_4Cl_2$) was used as the detecting oil. The sliding behavior, as well as the oil droplet transportation, was investigated by the contact-angle system and a charge-coupled device camera system. For the process of underwater oil microdroplet transportation, the density of the water solution could be increased by adding sugar water into the glass container slowly or be diluted by adding deionized water. In order to speed up the transportation process, sugar water with a density of about 1.52 g cm^{-3} was prepared in advance by dissolving sugar into deionized water.

Supporting Information

Supporting Information is available from the Wiley Online Library or from the author.

Acknowledgements

This work is supported by the National Science Foundation of China under the grant nos. 61275008, 61176113, and 51335008, the Special-funded programme on the national key scientific instruments and equipment development of China under the grant no. 2012YQ12004706.

Received: August 22, 2014
Revised: September 22, 2014
Published online: November 2, 2014

[1] F. Xia, L. Jiang, *Adv. Mater.* **2008**, *20*, 2842.
[2] T. L. Sun, G. Y. Qing, *Adv. Mater.* **2011**, *23*, H57.
[3] X. Yao, Y. L. Song, L. Jiang, *Adv. Mater.* **2011**, *23*, 719.
[4] K. S. Liu, L. Jiang, *Nano Today* **2011**, *6*, 155.
[5] Y. L. Zhang, H. Xia, E. Kim, H. B. Sun, *Soft Matter* **2012**, *8*, 11217.
[6] J. L. Yong, Q. Yang, F. Chen, D. S. Zhang, U. Farooq, G. Q. Du, X. Hou, *J. Mater. Chem. A* **2014**, *2*, 5499.
[7] C. M. Ding, Y. Zhu, M. J. Liu, L. Feng, M. X. Wan, L. Jiang, *Soft Matter* **2012**, *8*, 9064.
[8] B. Zhao, J. S. Moore, D. J. Beebe, *Science* **2001**, *291*, 1023.
[9] B. P. Casavant, E. Berthier, A. B. Theberge, J. Berthier, S. I. Montanez-Sauri, L. L. Bischel, K. Brakke, C. J. Hedman, W. Bushman, N. P. Keller, D. J. Beebe, *Proc. Natl. Acad. Sci. USA* **2013**, *110*, 10111.
[10] H. Mertaniemi, V. Jokinen, L. Sainiemi, S. Franssila, A. Marmur, O. Ikkala, R. H. A. Ras, *Adv. Mater.* **2011**, *23*, 2911.
[11] W. Barthlott, C. Neinhuis, *Planta* **1997**, *202*, 1.
[12] J. L. Yong, Q. Yang, F. Chen, D. S. Zhang, G. Q. Du, J. H. Si, F. Yun, X. Hou, *J. Micromech. Microeng.* **2014**, *24*, 035006.
[13] L. Feng, Y. N. Zhang, J. M. Xi, Y. Zhu, N. Wang, F. Xia, L. Jiang, *Langmuir* **2008**, *24*, 4114.
[14] J. L. Yong, F. Chen, Q. Yang, D. S. Zhang, G. Q. Du, J. H. Si, F. Yun, X. Hou, *J. Phys. Chem. C* **2013**, *117*, 24907.
[15] Y. Zhao, J. Fang, H. X. Wang, X. G. Wang, T. Lin, *Adv. Mater.* **2010**, *22*, 707.
[16] M. H. Jin, X. J. Feng, L. Feng, T. L. Sun, J. Zhai, T. J. Li, L. Jiang, *Adv. Mater.* **2005**, *17*, 1997.
[17] Y. K. Lai, X. F. Gao, H. F. Zhuang, J. Y. Huang, C. J. Lin, L. Jiang, *Adv. Mater.* **2009**, *21*, 3799.
[18] X. Hong, X. F. Gao, L. Jiang, *J. Am. Chem. Soc.* **2007**, *129*, 1478.
[19] Z. J. Chen, L. Feng, L. Jiang, *Adv. Funct. Mater.* **2008**, *18*, 3219.
[20] D. Wu, S. Z. Wu, Q. D. Chen, Y. L. Zhang, J. Yao, X. Yao, L. G. Niu, J. N. Wang, L. Jiang, H. B. Sun, *Adv. Mater.* **2011**, *23*, 545.
[21] A. Tuteja, W. Choi, M. Ma, J. M. Mabry, S. A. Mazzella, G. C. Rutledge, G. H. McKinley, R. E. Cohen, *Science* **2007**, *318*, 1618.
[22] T. S. Wong, S. H. Kang, S. K. Y. Tang, E. J. Smythe, B. D. Hatton, A. Grinthal, J. Aizenberg, *Nature* **2011**, *447*, 443.
[23] X. Deng, L. Manmen, H. J. Butt, D. Vollmer, *Science* **2012**, *335*, 67.
[24] K. Li, J. Ju, Z. X. Xue, J. Ma, L. Feng, S. Gao, L. Jiang, *Nat. Commun.* **2013**, *4*, 2276.
[25] M. J. Liu, S. T. Wang, Z. X. Wei, Y. L. Song, L. Jiang, *Adv. Mater.* **2009**, *21*, 665.
[26] X. L. Liu, J. Zhou, Z. X. Xue, J. Gao, J. X. Meng, S. T. Wang, L. Jiang, *Adv. Mater.* **2012**, *24*, 3401.
[27] M. H. Jin, S. S. Li, J. Wang, Z. X. Xue, M. Y. Liao, S. T. Wang, *Chem. Commun.* **2012**, *48*, 11745.
[28] Z. X. Xue, M. J. Liu, L. Feng, *J. Polym. Sci. Part B: Polym. Phys.* **2012**, *50*, 1209.
[29] Z. X. Xue, Y. Z. Cao, N. Liu, L. Feng, L. Jiang, *J. Mater. Chem. A* **2014**, *2*, 2445.
[30] M. Paven, P. Papadopoulos, S. Schöttle, X. Deng, V. Mailänder, D. Vollmer, H. J. Butt, *Nat. Commun.* **2013**, *4*, 2512.
[31] F. Zhang, W. B. Zhang, Z. Shi, D. Wang, J. Jin, L. Jiang, *Adv. Mater.* **2013**, *25*, 4192.
[32] X. L. Liu, J. Gao, Z. X. Xue, L. Chen, L. Li, L. Jiang, S. T. Wang, *ACS Nano* **2012**, *6*, 5614.
[33] D. Wu, S. Z. Wu, Q. D. Chen, S. Zhao, H. Zhang, J. Jiao, J. A. Piersol, J. N. Wang, H. B. Sun, L. Jiang, *Lab Chip* **2011**, *11*, 3873.
[34] X. F. Gao, L. P. Xu, Z. X. Xue, L. Feng, J. T. Peng, Y. Q. Wen, S. T. Wang, X. J. Zhang, *Adv. Mater.* **2014**, *26*, 1771.
[35] G. N. Ju, M. J. Cheng, F. Shi, *NPG Asia Mater.* **2014**, *6*, e111.
[36] M. J. Cheng, G. N. Ju, C. Jiang, Y. J. Zhang, F. Shi, *J. Mater. Chem. A* **2013**, *1*, 13411.
[37] G. N. Ju, M. J. Cheng, M. Xiao, J. M. Xu, K. Pan, X. Wang, Y. J. Zhang, F. Shi, *Adv. Mater.* **2013**, *25*, 2915.
[38] F. Chen, D. S. Zhang, Q. Yang, X. H. Wang, B. J. Dai, X. M. Li, X. Q. Hao, Y. C. Ding, J. H. Si, X. Hou, *Langmuir* **2011**, *27*, 359.
[39] D. S. Zhang, F. Chen, Q. Yang, J. H. Si, X. Hou, *Soft Matter* **2011**, *7*, 8337.
[40] J. L. Yong, F. Chen, Q. Yang, D. S. Zhang, H. Bian, G. Q. Du, J. H. Si, X. W. Meng, X. Hou, *Langmuir* **2013**, *29*, 3274.
[41] Q. Wen, J. C. Di, L. Jiang, J. H. Yu, R. R. Xu, *Chem. Sci.* **2013**, *4*, 591.